

Robust virtual element methods for 3D stress-assisted diffusion problems

Andrés E. Rubiano*

February 5, 2025

Abstract

This paper presents an initial exploration of stress-assisted diffusion problems in three dimensions within the framework of the virtual element method (VEM). Hilbert spaces enriched with parameter-weighted norms, the extended Babuška–Brezzi–Braess theory for perturbed saddle-point problems, and Banach fixed-point theory play a crucial role in performing a robust analysis of the fully coupled nonlinear system. The proposed virtual element formulations are provided with appropriate projection, interpolation, and stabilisation operators that ensures the well-posedness of the discrete problem. Numerical simulations are conducted to show the accuracy, performance, and applicability of the method.

2020 MSC codes: 65N99; 65Y99.

Keywords: virtual element methods, stress-assisted diffusion, diffusion-induced stress, perturbed saddle-point problems.

1 Introduction

Scope. Stress-assisted diffusion appears broadly in applications like Lithium-ion battery cells, silicon rubber and hydrogen diffusion, polymer-based coatings, semiconductor fabrication, oxidation of silicon nanostructures, and enhancing of conductivity properties in soft living tissue. In these processes, the stress of the material involved affects the patterns of diffusion. This

*School of Mathematics, Monash University, 9 Rainforest Walk, 3800 VIC, Australia.
andres.rubianomartinez@monash.edu, <https://orcid.org/0000-0002-5557-4963>

paper addresses one of the simplest models for such an interaction, incorporating stress effects inside the diffusion coefficient, and recovering Fick's law in the absence of these phenomena (see, e.g., [4]). Moreover, we extend the analysis done in [8] pointing out the definition of VEM spaces in 3D and the polynomial, interpolation, and stabilisation operators used in this framework.

Outline. The content of the paper is organised as follows: The remainder of this section presents the strong form of the coupled fully coupled stress-assisted diffusion problem. Section 2 is devoted to presenting the weak formulation and well-posedness analysis using perturbed saddle-point theory and fixed-point arguments. In Section 3 we define the discrete problem, show the existence and uniqueness of discrete solution, and outline the a priori error analysis. Finally, in Section 4 we provide numerical results that illustrate the theoretical results presented, and we present as an application of the model the lithiation of a perforated cylindrical anode particle.

Model statement. Let us consider the following nonlinear formulation for stress-assisted diffusion of a solute that interacts with an elastic material

$$-\operatorname{div}(2\mu\boldsymbol{\varepsilon}(\mathbf{u}) - p\mathbb{I}) = \mathbf{f} \quad \text{in } \Omega, \quad \mathbf{u} = \mathbf{0} \quad \text{on } \Gamma_D, \quad (1.1a)$$

$$p = -\lambda \operatorname{div} \mathbf{u} + \ell(\varphi) \quad \text{in } \Omega, \quad (2\mu\boldsymbol{\varepsilon}(\mathbf{u}) - p\mathbb{I})\mathbf{n} = \mathbf{0} \quad \text{on } \Gamma_N, \quad (1.1b)$$

$$\boldsymbol{\zeta} = \mathbb{M}(\boldsymbol{\varepsilon}(\mathbf{u}), p)\nabla\varphi \quad \text{in } \Omega, \quad \varphi = \varphi_D \quad \text{on } \Gamma_D, \quad (1.1c)$$

$$\theta\varphi - \operatorname{div}(\boldsymbol{\zeta}) = g \quad \text{in } \Omega, \quad \boldsymbol{\zeta} \cdot \mathbf{n} = 0 \quad \text{on } \Gamma_N. \quad (1.1d)$$

Equations (1.1a) and (1.1b) constitute a Herrmann-like mixed formulation for linear elasticity. The coupling between the displacement \mathbf{u} of the material, the pressure p , and the solute concentration φ follows Hooke's law to express the Cauchy stress tensor as $2\mu\boldsymbol{\varepsilon}(\mathbf{u}) - p\mathbb{I}$, μ and λ are the Lamé parameters, ℓ is the active stress coefficient, and \mathbf{f} is a vector of external body loads.

On the other hand, equations (1.1d) and (1.1c) correspond to the reaction-diffusion equation written in mixed form where $\boldsymbol{\zeta}$ is the diffusive flux, g is a given net volumetric source of solute, θ is a positive model parameter, and $\mathbb{M}(\boldsymbol{\varepsilon}(\mathbf{u}), p)$ is the stress-assisted diffusion coefficient.

We adopt mixed loading boundary conditions for the coupled problem: the structure is clamped and has a given concentration on Γ_D , where the boundary subset $\Gamma_D \subset \partial\Omega$ is of positive surface measure. In addition, a given traction and zero solute flux are prescribed on $\Gamma_N := \partial\Omega \setminus \Gamma_D$.

The nonlinear terms. We assume that $\mathbb{M}(\cdot, \cdot)$ is symmetric, positive semi-definite and uniformly bounded in $\mathbb{L}^\infty(\Omega)$, likewise for $\mathbb{M}^{-1}(\cdot, \cdot)$. More ex-

plicitly, for all $\mathbf{w} \in \mathbf{H}^1(\Omega)$, $r \in L^2(\Omega)$ and $\mathbf{x}, \mathbf{y} \in \mathbb{R}^3$ there exists $M \in \mathbb{R}$ such that $0 < M^{-1} \leq M$ with $M^{-1}\mathbf{x} \cdot \mathbf{x} \leq \mathbf{x} \cdot [\mathbb{M}^{-1}(\boldsymbol{\varepsilon}(\mathbf{w}), r)\mathbf{x}]$, and $\mathbf{y} \cdot [\mathbb{M}^{-1}(\boldsymbol{\varepsilon}(\mathbf{w}), r)\mathbf{x}] \leq M\mathbf{x} \cdot \mathbf{y}$. In addition, we assume that $\ell : L^2(\Omega) \rightarrow L^2(\Omega)$ and satisfies $\|\ell(\vartheta)\|_{0,\Omega} \lesssim \|\vartheta\|_{0,\Omega}$ for all $\vartheta \in L^2(\Omega)$. Moreover, we assume that $\mathbb{M}^{-1}(\cdot, \cdot)$ and $\ell(\cdot)$ are Lipschitz continuous with Lipschitz constants $L_{\mathbb{M}}$ and L_ℓ . Examples of these terms can be found in [7] for the stress-assisted diffusion and [10] for the active stress.

2 Weak formulation

In view of the boundary conditions, we define the Hilbert spaces

$$\begin{aligned} \mathbf{H}_D^1(\Omega) &:= \{\mathbf{v} \in \mathbf{H}^1(\Omega) : \mathbf{v} = \mathbf{0} \text{ on } \Gamma_D\}, \\ \mathbf{H}_N(\text{div}, \Omega) &:= \{\boldsymbol{\xi} \in \mathbf{H}(\text{div}, \Omega) : \boldsymbol{\xi} \cdot \mathbf{n} = 0 \text{ on } \Gamma_N\}, \end{aligned}$$

with the boundary assignment understood in the sense of traces, and consider the following weak formulation: for given $\mathbf{f} \in \mathbf{L}^2(\Omega)$, $g \in L^2(\Omega)$, and $\varphi_D \in H^{1/2}(\Gamma_D)$, find $(\mathbf{u}, p, \boldsymbol{\zeta}, \varphi) \in \mathbf{H}_D^1(\Omega) \times L^2(\Omega) \times \mathbf{H}_N(\text{div}, \Omega) \times L^2(\Omega)$ such that

$$2\mu \int_{\Omega} \boldsymbol{\varepsilon}(\mathbf{u}) : \boldsymbol{\varepsilon}(\mathbf{v}) - \int_{\Omega} p \text{div } \mathbf{v} = \int_{\Omega} \mathbf{f} \cdot \mathbf{v}, \quad \forall \mathbf{v} \in \mathbf{H}_D^1(\Omega) \quad (2.1a)$$

$$- \int_{\Omega} q \text{div } \mathbf{u} - \lambda^{-1} \int_{\Omega} pq = \lambda^{-1} \int_{\Omega} \ell(\varphi)q, \quad \forall q \in L^2(\Omega) \quad (2.1b)$$

$$\int_{\Omega} \mathbb{M}(\boldsymbol{\varepsilon}(\mathbf{u}), p)^{-1} \boldsymbol{\zeta} \cdot \boldsymbol{\xi} + \int_{\Omega} \varphi \text{div } \boldsymbol{\xi} = \langle \varphi_D, \boldsymbol{\xi} \cdot \mathbf{n} \rangle_{\Gamma_D}, \quad \forall \boldsymbol{\xi} \in \mathbf{H}_N(\text{div}, \Omega) \quad (2.1c)$$

$$\int_{\Omega} \psi \text{div } \boldsymbol{\zeta} - \theta \int_{\Omega} \varphi \psi = - \int_{\Omega} g\psi, \quad \forall \psi \in L^2(\Omega). \quad (2.1d)$$

Unique solvability with parameter-weighted norms. Let us adopt the following notation for the functional spaces for displacement and total volumetric stress $\mathbf{V}_1 := \mathbf{H}_D^1(\Omega)$ and $Q_1 = Q_{b_1} := L^2(\Omega)$, equipped with the scaled norms and semi-norms given by

$$\begin{aligned} \|\mathbf{u}\|_{\mathbf{V}_1}^2 &:= 2\mu \|\boldsymbol{\varepsilon}(\mathbf{u})\|_{0,\Omega}^2, & \|p\|_{Q_1}^2 &:= ((2\mu)^{-1} + \lambda^{-1}) \|p\|_{0,\Omega}^2, \\ |\mathbf{v}|_{1,\mathbf{V}_1}^2 &:= 2\mu |\mathbf{v}|_{1,\Omega}^2, & |q|_{1,Q_{b_1}}^2 &:= (2\mu)^{-1} |q|_{1,\Omega}^2. \end{aligned}$$

On the other hand, let us denote the functional spaces for diffusive flux and concentration as $\mathbf{V}_2 = \mathbf{H}_N(\text{div}, \Omega)$ and $Q_2 = Q_{b_2} := L^2(\Omega)$, furnished with

the following norms and semi-norms as $\|\boldsymbol{\zeta}\|_{\mathbb{M},\Omega}^2 := \int_{\Omega} \mathbb{M}(\boldsymbol{\varepsilon}(\mathbf{u}), p)^{-1} \boldsymbol{\zeta} \cdot \boldsymbol{\zeta}$,

$$\begin{aligned} \|\boldsymbol{\zeta}\|_{\mathbf{V}_2}^2 &:= \|\boldsymbol{\zeta}\|_{\mathbb{M},\Omega}^2 + M \|\operatorname{div} \boldsymbol{\zeta}\|_{0,\Omega}^2, & \|\varphi\|_{Q_2}^2 &:= (M^{-1} + \theta) \|\varphi\|_{0,\Omega}^2, \\ |\boldsymbol{\xi}|_{1,\mathbf{V}_2}^2 &:= M |\boldsymbol{\xi}|_{1,\Omega}^2, & |\psi|_{1,Q_{b_2}}^2 &:= M^{-1} |\psi|_{1,\Omega}^2. \end{aligned}$$

The proposed spaces in conjunction with the extended Babuška–Brezzi–Braess theory for perturbed saddle-point problems and a fixed-point argument show the robust unique solvability of our weak formulation presented in Section 2. We finish this section by stating the continuous dependence on data (see [8, Section 3] for details).

Theorem 1. *Let $W = \{w \in Q_2: \|w\|_{Q_2} \leq C_2 \sqrt{M} \|\varphi_D\|_{1/2,\Gamma_D} + \|g\|_{0,\Omega}\}$. Under the assumptions over the non-linear terms, suppose further that $1 \leq \lambda$, $1 \leq \mu$, $\theta \leq M^{-1}$, and $C_1 L \ell \sqrt{2\mu} M^2 C_2^2 L_{\mathbb{M}} (\|\varphi_D\|_{1/2,\Gamma_D} + \|g\|_{0,\Omega}) < 1$. Then, for $\varphi \in W$ there is a unique solution $(\mathbf{u}, p, \boldsymbol{\zeta}, \varphi) \in \mathbf{V}_1 \times Q_1 \times \mathbf{V}_2 \times Q_2$ of (2.1) such that*

$$\|(\mathbf{u}, p)\|_{\mathbf{V}_1 \times Q_1} \leq C_1 (\|F_1\|_{\mathbf{V}_1} + \|G_1^{\varphi}\|_{Q_1}), \quad (2.2a)$$

$$\|(\boldsymbol{\zeta}, \varphi)\|_{\mathbf{V}_2 \times Q_2} \leq C_2 (\|F_2\|_{\mathbf{V}_2} + \|G_2\|_{Q_2}), \quad (2.2b)$$

where the constants C_1 and C_2 do not depend on the physical parameters.

3 Virtual element discretisation

Mesh assumptions. Let \mathcal{T}^h be a decomposition of Ω into polyhedral elements P with diameter h_P , let \mathcal{F}^h be the set of faces f with length h_f and \mathcal{E}^h be the set of edges e of \mathcal{T}^h with length h_e . The following mesh assumptions are considered throughout this paper. We assume that there exists a universal constant $\rho > 0$ such that

- (M1) Each polyhedral element P is star-shaped with respect to a ball of radius $\geq \rho h_P$,
- (M2) Every face f of P is of diameter h_f and is star-shaped with respect to a disk of radius $\geq \rho h_P$,
- (M3) Every edge e of P has length $\geq \rho h_P$.

Polynomial spaces. Given an integer $k \geq 0$ the space of polynomials of degree $\leq k$ on P is denoted by $\mathcal{P}_k(P)$ (resp. for faces f). The space of the gradients of polynomials of grade $\leq k + 1$ on P is denoted as $\mathcal{G}_k(P) :=$

$\nabla(\mathcal{P}_{k+1}(P))$ with standard notation $\mathcal{P}_{-1}(P) = \{0\}$ for $k = -1$. The space $\mathcal{G}_k^\oplus(P)$ denotes the complement of the space $\mathcal{G}_k(P)$ in the vector polynomial space $(\mathcal{P}_k(P))^3$, that is, $(\mathcal{P}_k(P))^3 = \mathcal{G}_k(P) \oplus \mathcal{G}_k^\oplus(P)$. In particular, following [2], we set $\mathcal{G}_k^\oplus(P) := \mathbf{x} \wedge (\mathcal{P}_{k-1}(P))^3$ with $\mathbf{x} = (x_1, x_2, x_3)^\top$. Likewise, the space that defines the rotational of polynomials with degree $\leq k+1$ is denoted as $\mathcal{R}_k(P) := \mathbf{curl}(\mathcal{P}_{k+1}(P))$ where the associated complement space $\mathcal{R}_k^\oplus(P)$ fulfills the property $(\mathcal{P}_k(P))^3 = \mathcal{R}_k(P) \oplus \mathcal{R}_k^\oplus(P)$ with $\mathcal{R}_k^\oplus(P) = \mathbf{x} \mathcal{P}_{k-1}(P)$.

Let $\mathbf{x}_P = (x_{1,P}, x_{2,P}, x_{3,P})^\top$ denote the barycentre of P and let $\mathcal{M}_k(P)$ be the set of scaled monomials

$$\mathcal{M}_k(P) := \left\{ \left(\frac{\mathbf{x} - \mathbf{x}_P}{h_P} \right)^\alpha, 0 \leq |\alpha| \leq k \right\},$$

where $\alpha = (\alpha_1, \alpha_2, \alpha_3)^\top$ is a non-negative multi-index with $|\alpha| = \alpha_1 + \alpha_2 + \alpha_3$ and $\mathbf{x}^\alpha = x_1^{\alpha_1} x_2^{\alpha_2} x_3^{\alpha_3}$. In particular, we can take the basis of $\mathcal{G}_k(P)$ and $\mathcal{G}_k^\oplus(P)$ as $\mathcal{M}_k^\nabla(P) := \nabla \mathcal{M}_{k+1}(P) \setminus \{0\}$ and $\mathcal{M}_k^\oplus(P) := \mathbf{x}_P \wedge (\mathcal{M}_{k-1}(P))^3$, where $(\mathcal{M}_k(P))^3 = \mathcal{M}_k^\nabla(P) \oplus \mathcal{M}_k^\oplus(P)$ holds. In addition, we introduce the notation $\mathcal{M}_{k \setminus k-1}(P) := \mathcal{M}_k(P) \setminus \mathcal{M}_{k-1}(P)$.

Discrete formulation for the elasticity problem. The definition of the enhanced 3D VE space follows the approach for Stokes-like problems given in [3]. Given $k_1 \geq 2$. First, we define an extended enhance local VE space as

$$\begin{aligned} \mathbf{V}_1^{h,k_1}(P) := & \{ \mathbf{v}_h \in \mathbf{H}^1(P) : \mathbf{v}_h|_{\partial P} \in (\tilde{\mathcal{B}}_1^{h,k_1}(\partial P))^3, \operatorname{div} \mathbf{v}_h \in \mathcal{P}_{k_1-1}(P), \\ & - 2\mu \operatorname{div} \boldsymbol{\varepsilon}(\mathbf{v}_h) - \nabla s \in \mathcal{G}_{k_1}^\oplus(P) \text{ for some } s \in L_0^2(P), \\ & \int_P (\mathbf{v}_h - \Pi_1^{\boldsymbol{\varepsilon},k_1} \mathbf{v}_h) \cdot \mathbf{m}_{k_1}^\oplus = 0, \forall \mathbf{m}_{k_1}^\oplus \in \mathcal{M}_{k_1 \setminus k_1-2}^\oplus(P) \}, \end{aligned}$$

where the boundary space of VE functions along the boundary ∂P of P , is defined as follows

$$\tilde{\mathcal{B}}_1^{h,k_1}(\partial P) := \{ v_h \in C^0(\partial P) : v_h|_f \in \tilde{\mathcal{B}}_1^{h,k_1}(f), \forall f \subset \partial P \},$$

and for each face $f \in \partial P$, the enhanced VE space $\tilde{\mathcal{B}}_1^{h,k_1}(f)$ locally solves the Poisson equation with Dirichlet boundary conditions and is defined by

$$\begin{aligned} \tilde{\mathcal{B}}_1^{h,k_1}(f) := & \{ v_h \in H^1(f) : v_h|_{\partial f} \in C^0(\partial f), v|_e \in \mathcal{P}_{k_1}(e), \Delta_f v_h \in \mathcal{P}_{k_1+1}(f), \\ & \int_f (v_h - \Pi_1^{\boldsymbol{\varepsilon},k_1,f} v_h) m_{k_1+1} = 0, \forall e \subset \partial f, \forall m_{k_1+1} \in \mathcal{M}_{k_1+1 \setminus k_1-2}(f) \}, \end{aligned}$$

where Δ_f denotes the tangential differential operator on f , $\Pi_1^{\boldsymbol{\varepsilon},k_1,f}$ is the restriction to the face f of the energy projection operator for scalar functions

defined in (3.1). The global discrete spaces are set as

$$\begin{aligned}\mathbf{V}_1^{h,k_1} &:= \{\mathbf{v}_h \in \mathbf{V}_1 : \mathbf{v}_h|_P \in \mathbf{V}_1^{h,k_1}(P), \forall P \in \mathcal{T}^h\}, \\ Q_1^{h,k_1} &:= \{q_h \in Q_1 : q_h|_P \in \mathcal{P}_{k_1-1}(P), \forall P \in \mathcal{T}^h\}.\end{aligned}$$

Discrete formulation for the reaction-diffusion problem. The construction of $\mathbf{H}(\text{div}, \Omega)$ conforming 3D VE space naturally follows the same approach as its 2D counterpart. For further details, we refer the reader to [1]. In this case, we differ from the 2D version by setting $k_2 \geq 1$. The discrete VE space locally solve a $\nabla(\text{div}) - \text{curl}$ problem as follows

$$\begin{aligned}\mathbf{V}_2^{h,k_2}(P) &:= \{\boldsymbol{\xi}_h \in \mathbf{H}(\text{div}, P) \cap \mathbf{H}(\text{curl}, P) : \boldsymbol{\xi}_h \cdot \mathbf{n}_P^f|_f \in \mathcal{P}_{k_2}(f), \forall f \in \partial P, \\ &\quad \nabla(\text{div } \boldsymbol{\xi}_h) \in \mathcal{G}_{k_2-2}(P), \text{curl } \boldsymbol{\xi}_h \in \mathcal{R}_{k_2-1}(P)\}.\end{aligned}$$

Then, the discrete global spaces are defined by

$$\begin{aligned}\mathbf{V}_2^{h,k_2} &:= \{\boldsymbol{\xi}_h \in \mathbf{V}_2 : \boldsymbol{\xi}_h|_P \in \mathbf{V}_2^{h,k_2}(P), \forall P \in \mathcal{T}^h\}, \\ Q_2^{h,k_2} &:= \{\psi_h \in Q_2 : \psi_h|_P \in \mathcal{P}_{k_2-1}(P), \forall P \in \mathcal{T}^h\}.\end{aligned}$$

Polynomial projections. The energy projection operator given by $\Pi_1^{\varepsilon,k_1} : \mathbf{H}^1(P) \rightarrow (\mathcal{P}_{k_1}(P))^3$, and the L^2 -projections operators defined as $\Pi_j^{0,k_j} : L^2(P) \rightarrow (\mathcal{P}_{k_j}(P))^3$ with $j = 1, 2$ fulfill that

$$\bullet \left\{ \begin{aligned} \int_P \boldsymbol{\varepsilon}(\mathbf{v}_h - \Pi_1^{\varepsilon,k_1} \mathbf{v}_h) : \boldsymbol{\varepsilon}(\mathbf{m}_{k_1}) &= 0, \quad \forall \mathbf{m}_{k_1} \in (\mathcal{M}_{k_1}(P))^3, \\ \int_{\partial P} (\Pi_1^{\varepsilon,k_1} \mathbf{v} - \mathbf{v}) \cdot \mathbf{m}_{\text{RBM}} &= 0, \quad \forall \mathbf{m}_{\text{RBM}} \in \text{RBM}(P), \end{aligned} \right. \quad (3.1)$$

$$\bullet \int_P (\mathbf{v}_h - \Pi_j^{0,k_j} \mathbf{v}_h) \cdot \mathbf{m}_{k_j} = 0, \quad \forall \mathbf{m}_{k_j} \in (\mathcal{M}_{k_j}(P))^3, \quad (3.2)$$

where $\text{RBM}(P)$ denotes the set of scaled rigid body motions. We recall that the definition for scalar functions is analogous with the usual notation Π_1^{ε,k_1} and Π_j^{0,k_j} for $j = 1, 2$. Regarding computability, we refer the reader to [3, Proposition 5.1] and [1, Theorem 3.2].

Interpolation operators. Let $1/2 < s_1 \leq k_1$, $0 \leq s_2 \leq k_2$. The Fortin-like (see [6, 9]) interpolation operators $\Pi_1^{F,k_1} : \mathbf{H}^{s_1+1}(P) \rightarrow \mathbf{V}_1^{h,k_1}(P)$, and $\Pi_2^{F,k_2} : \mathbf{H}^{s_2+1}(P) \rightarrow \mathbf{V}_2^{h,k_2}(P)$ are defined through the Degrees of freedom as

$$\bullet \text{DoF}_j(\mathbf{v} - \Pi_j^{F,k_j} \mathbf{v}) = 0, \quad \forall \mathbf{v} \in \mathbf{H}^{s_j+1}(P), \quad j = 1, \dots, \dim(\mathbf{V}_j^{h,k_j}(P)),$$

where the operator DoF_j indicates the application of the j -th Degree of Freedom (see [1, 3]). Note that the associated commutative property is given as $\text{div } \Pi_j^{F,k_j}(\cdot) = \Pi_j^{0,k_j-1} \text{div}(\cdot)$.

Approximation and interpolation estimates. This paragraph collects all the results involving approximation and interpolation estimates needed for the discrete formulation. We recall that arise as consequence of classical estimates and for the robust version of the estimates we refer to [8, Section 4] pointing out that the extension to the 3D estimates follow similarly.

Lemma 1. *For any $\mathbf{v} \in (\mathbf{H}^{s_1+1}(P) \cap \mathbf{V}_1(P), |\cdot|_{1,\mathbf{V}_1(P)})$, $q \in (H^{s_1+1}(P) \cap Q_{b_1}(P), |\cdot|_{1,Q_{b_1}(P)})$, $\boldsymbol{\xi} \in (\mathbf{H}^{s_2+1}(P) \cap \mathbf{V}_2(P), |\cdot|_{1,\mathbf{V}_2(P)})$ and $\psi \in (H^{s_2+1}(P) \cap Q_{b_2}(P), |\cdot|_{1,Q_{b_2}(P)})$, the polynomial projections $\Pi_1^{\varepsilon,k_1} \mathbf{v}$, $\Pi_1^{0,k_1} q$, $\Pi_2^{0,k_2} \boldsymbol{\xi}$ and $\Pi_2^{0,k_2} \psi$ satisfy the following estimates*

$$\begin{aligned} \|\mathbf{v} - \Pi_1^{\varepsilon,k_1} \mathbf{v}\|_{\mathbf{V}_1(P)} &\lesssim h_P^{s_1} |\mathbf{v}|_{\mathbf{V}_1(P)}, & \|q - \Pi_1^{0,k_1} q\|_{Q_{b_1}(P)} &\lesssim h_P^{s_1+1} |q|_{Q_{b_1}(P)}, \\ \|\boldsymbol{\xi} - \Pi_2^{0,k_2} \boldsymbol{\xi}\|_{\mathbb{M},P} &\lesssim h_P^{s_2+1} |\boldsymbol{\xi}|_{\mathbf{V}_2(P)}, & \|\psi - \Pi_2^{0,k_2} \psi\|_{Q_{b_2}(P)} &\lesssim h_P^{s_2+1} |\psi|_{Q_{b_2}(P)}. \end{aligned}$$

Lemma 2. *Given $\mathbf{v} \in (\mathbf{H}^{s_1+1}(P) \cap \mathbf{V}_1(P), |\cdot|_{1,\mathbf{V}_1(P)})$ and $\boldsymbol{\xi} \in (\mathbf{H}^{s_2+1}(P) \cap \mathbf{V}_2(P), |\cdot|_{1,\mathbf{V}_2(P)})$. The Fortin interpolation operators Π_1^{F,k_1} and Π_2^{F,k_2} satisfy*

$$\|\mathbf{v} - \Pi_1^{F,k_1} \mathbf{v}\|_{\mathbf{V}_1(P)} \lesssim h_P^{s_1} |\mathbf{v}|_{1,\mathbf{V}_1(P)}, \quad \|\boldsymbol{\xi} - \Pi_2^{F,k_2} \boldsymbol{\xi}\|_{\mathbb{M},P} \lesssim h_P^{s_2+1} |\boldsymbol{\xi}|_{1,\mathbf{V}_2(P)}.$$

The virtual element formulation for the stress-assisted diffusion problem. The discrete formulation for the fully-coupled problem reads: For given $\mathbf{f} \in \mathbf{L}^2(\Omega)$, $g \in L^2(\Omega)$, and $\varphi_D \in H^{1/2}(\Gamma_D)$, find $(\mathbf{u}_h, p_h, \boldsymbol{\zeta}_h, \varphi_h) \in \mathbf{V}_1^{h,k_1} \times Q_1^{h,k_1} \times \mathbf{V}_2^{h,k_2} \times Q_2^{h,k_2}$ such that

$$\begin{aligned} \sum_{P \in \mathcal{T}^h} \left[2\mu \int_P \boldsymbol{\varepsilon}(\bar{\mathbf{u}}_h) : \boldsymbol{\varepsilon}(\bar{\mathbf{v}}_h) + S_1^P(\mathbf{u}_h - \bar{\mathbf{u}}_h, \mathbf{v}_h - \bar{\mathbf{v}}_h) - \int_\Omega p_h \operatorname{div} \mathbf{v}_h \right] \\ = \sum_{P \in \mathcal{T}^h} \int_P \bar{\mathbf{f}} \cdot \mathbf{v}_h, \quad \forall \mathbf{v}_h \in \mathbf{V}_1^{h,k_1}, \end{aligned} \quad (3.3a)$$

$$\sum_{P \in \mathcal{T}^h} \left[- \int_P q_h \operatorname{div} \mathbf{u}_h - \lambda^{-1} \int_P p_h q_h \right] = \sum_{P \in \mathcal{T}^h} \lambda^{-1} \int_P \ell(\varphi_h) q_h, \quad \forall q_h \in Q_1^{h,k_1}, \quad (3.3b)$$

$$\begin{aligned} \sum_{P \in \mathcal{T}^h} \left[\int_P \mathbb{M}(\bar{\mathbf{u}}_h, p_h)^{-1} \bar{\boldsymbol{\zeta}}_h \cdot \bar{\boldsymbol{\xi}}_h + S_2^{\bar{\mathbf{u}}_h, p_h, P}(\boldsymbol{\zeta}_h - \bar{\boldsymbol{\zeta}}_h, \boldsymbol{\xi}_h - \bar{\boldsymbol{\xi}}_h) + \int_P \varphi_h \operatorname{div} \boldsymbol{\xi}_h \right] \\ = \sum_{P \in \mathcal{T}^h} \langle \varphi_D, \boldsymbol{\xi}_h \cdot \mathbf{n} \rangle_{\partial P \cap \Gamma_D}, \quad \forall \boldsymbol{\xi}_h \in \mathbf{V}_2^{h,k_2}, \end{aligned} \quad (3.3c)$$

$$\sum_{P \in \mathcal{T}^h} \left[\int_P \psi_h \operatorname{div} \boldsymbol{\zeta}_h - \theta \int_\Omega \varphi_h \psi_h \right] = - \sum_{P \in \mathcal{T}^h} \int_P g \psi_h, \quad \forall \psi_h \in Q_2^{h,k_2}, \quad (3.3d)$$

with $\bar{\mathbf{u}}_h := \Pi_1^{\varepsilon, k_1} \mathbf{u}_h$, $\bar{\mathbf{v}}_h := \Pi_1^{\varepsilon, k_1} \mathbf{v}_h$, $\bar{\mathbf{f}} := \Pi_1^{0, k_1 - 2} \mathbf{f}$, $\bar{\boldsymbol{\zeta}}_h := \Pi_2^{0, k_2} \boldsymbol{\zeta}_h$, $\bar{\boldsymbol{\xi}}_h := \Pi_2^{0, k_2} \boldsymbol{\xi}_h$. The stabilisation terms are any symmetric and positive definite bilinear forms such that in the kernel of Π_1^{ε, k_1} (resp. Π_2^{0, k_2}) we have $\|\mathbf{v}_h\|_{\mathbf{V}_1} \lesssim S_1^E(\mathbf{v}_h, \mathbf{v}_h) \lesssim \|\mathbf{v}_h\|_{\mathbf{V}_1(P)}$, $\|\boldsymbol{\xi}_h\|_{\mathbb{M}, \Omega} \lesssim S_2^{\bar{\mathbf{u}}_h, p_h, E}(\boldsymbol{\xi}_h, \boldsymbol{\xi}_h) \lesssim \|\boldsymbol{\xi}_h\|_{\mathbb{M}, \Omega}$.

Similarly to the continuous case, the continuous dependence on data for (3.3) follows as an extension of [8, Section 4] (see Theorem 1), this is a consequence of the stabilisation operators, and the Fortin-like interpolation operators that lead to the discrete inf-sup condition. Note the associated constants \bar{C}_1, \bar{C}_2 that appear in the discrete well-posedness (independent of the physical parameters) do not need to coincide with C_1 , and C_2 . We finalise by recalling the convergence result of the VE scheme.

Theorem 2. *Under the assumptions of Theorem 1. Given $(\mathbf{u}, p, \boldsymbol{\zeta}, \varphi) \in (\mathbf{H}^{s_1+1}(\Omega) \cap \mathbf{V}_1) \times (H^{s_1}(\Omega) \cap Q_{b_1}) \times (\mathbf{H}^{s_2} \cap \mathbf{V}_2) \times (H^{s_2} \cap Q_{b_2})$, $(\mathbf{u}_h, p_h, \boldsymbol{\zeta}_h, \varphi_h) \in \mathbf{V}_1^{h, k_1} \times Q_1^{h, k_1} \times \mathbf{V}_2^{h, k_2} \times Q_2^{h, k_2}$ be the respective solutions of the continuous and discrete problems, with the data satisfying $\mathbf{f} \in \mathbf{H}^{s_1-1} \cap \mathbf{Q}_{b_1}$ and $g \in H^{s_2}(\Omega) \cap Q_{b_2}$. If $\bar{C}_1 \sqrt{M} L_\ell + \bar{C}_2 \sqrt{M^3} L_{\mathbb{M}} \sqrt{2\mu} (\|\varphi_D\|_{1/2, \Gamma_D} + \|g\|_{0, \Omega}) < 1/2$. Then, the total error $\bar{e}_h := \|(\mathbf{u} - \mathbf{u}_h, p - p_h, \boldsymbol{\zeta} - \boldsymbol{\zeta}_h, \varphi - \varphi_h)\|_{\mathbf{V}_1 \times Q_1 \times \mathbf{V}_2 \times Q_2}$ decays with the following rate for $s := \min\{s_1, s_2\}$*

$$\bar{e}_h \lesssim h^s (|\mathbf{f}|_{s_1-1, \mathbf{Q}_{b_1}} + |\mathbf{u}|_{s_1+1, \mathbf{V}_1} + |p|_{s_1, Q_{b_1}} + |g|_{s_2, Q_{b_2}} + |\boldsymbol{\zeta}|_{s_2, \mathbf{V}_2} + |\varphi|_{s_2, Q_{b_2}}).$$

4 Numerical results

The simulations presented are implemented in VEM++ [5] for lowest case order ($k_1 = 2, k_2 = 1$). The fixed point algorithm based on the analysis in [8] is optimised to ensure that, in each iteration, only the blocks containing non-linearities are reconstructed, improving the performance of the code. We recall that the computational error is computed as $\bar{e}_* := \|(\mathbf{u} - \bar{\mathbf{u}}_h, p - p_h, \boldsymbol{\zeta} - \bar{\boldsymbol{\zeta}}_h, \varphi - \varphi_h)\|_{\mathbf{V}_1 \times Q_1 \times \mathbf{V}_2 \times Q_2}$, and the fixed point tolerance is set to 10^{-5} .

Example 1. Let $\Omega = (0, 1)^3$ with $\Gamma_N = \{(x, y, z) \in \mathbb{R}^3 : x, y, z = 1\}$, and $\Gamma_D = \partial\Omega \setminus \Gamma_N$, we set the manufactured solutions as follows $\mathbf{u}(x, y, z) = (x^2 + x \cos(x) \sin(y), y^2 + x \cos(y) \sin(x), z^2 + x \cos(x) \cos(y)) / 5$, $\varphi(x, y, z) = \cos(\pi y) + \sin(\pi x) + x^2 + y^2 + z^2$, $\ell(\varphi) = 1 + \varphi^2 / (1 + \varphi^2)$, the non-linearities are given by $\mathbb{M}(\boldsymbol{\varepsilon}(\mathbf{u}), p) = 10^{-3} [e^{-10^{-4} \text{tr}((2\mu \boldsymbol{\varepsilon}(\mathbf{u}) - p)\mathbb{I})}] \mathbb{I}$, with the adimensional parameters $\mu = 10^2$, $\lambda = 10^3$, $\theta = 10^{-3}$, $M = 2 \times 10$. Figure 4 confirms the linear convergence rate as predicted in Theorem 2 for a variety of meshes, thanks to the flexibility provided by the VEM scheme proposed.

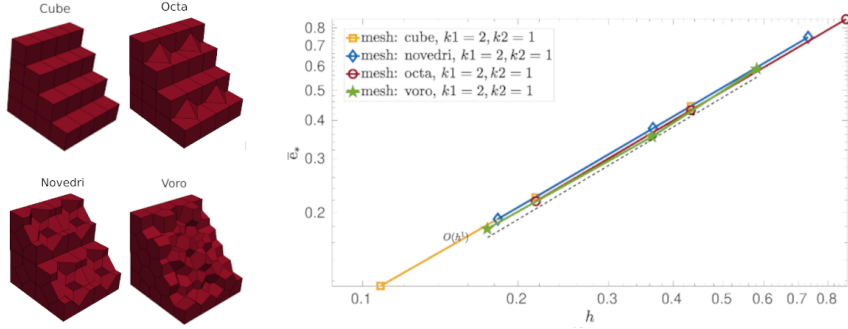


Figure 4.1: Example 1. An illustration of the distinct meshes used (left), and the converge plot under uniform refinement (right).

Example 2. The lithiation process is configured in a perforated cylindrical particle of outer radius of $5 \mu\text{m}$, inner radius of $1 \mu\text{m}$, and height of $5 \mu\text{m}$. The boundary conditions are given by: Clamped and zero lithium fluxes on the inner circumference, the maximum lithium concentration $\tilde{\Omega} = 2.29 \times 10^{-14} \text{ mol}/\mu\text{m}^3$ is fixed on the outer circumference, and a traction of $-2 \times 10^{-4} \text{ N}/\mu\text{m}^2$ on the outer circumference. The Young's modulus is given by $E = 1 \times 10^{-2} \text{ N}/\mu\text{m}^2$ and the Poisson ratio is $\nu = 0.3$. The diffusive source is zero and there is no body load force. The non-linear terms are given by $\mathbb{M}(\boldsymbol{\varepsilon}(\mathbf{u}), p) = m_0(\mathbb{I} + m_0 m_1((2\mu\boldsymbol{\varepsilon}(\mathbf{u}) - p)\mathbb{I})^2)$, and $\ell(\varphi) = K_0\varphi$, with $m_0 = 1 \times 10^2 \mu\text{m}^2/\text{s}$, $m_1 = 1 \times 10^3 \mu\text{m}^2/\text{N}$, $K_0 = \tilde{\Omega}(2\mu + 3\lambda)/3$ and the partial molar volume is $\tilde{\Omega} = 3.497 \times 10^{12} \mu\text{m}^3/\text{mol}$. Finally, $\theta = M = 1$. In this experiment, we checked the behaviour of the solution when the top and bottom bases were unclamped and clamped (see Figure 4), the results coincide with the behaviour expected (see e.g. [11]), confirming the applicability of the model.

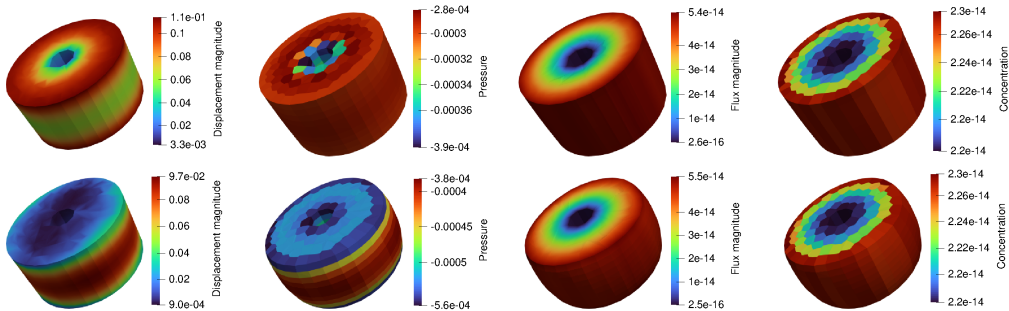


Figure 4.2: Example 2. Snapshots of the variables of interest in the reference configuration (left column), and deformed configuration (remaining columns) for the unclamped (first row), and clamped cases (second row).

Acknowledgements. This work has been partially supported by the Australian Research Council through the Future Fellowship Grant FT220100496. The author also thanks Prof. Ricardo Ruiz-Baier, Dr. Rekha Khot, and A/Prof. Franco Dassi for their constant support and expert guidance.

References

- [1] L. Beirão da Veiga, F. Brezzi, L. D. Marini, and A. Russo. $H(\text{div})$ and $H(\text{curl})$ -conforming VEM. *Numerische Mathematik*, 133:303–332, 06 2016.
- [2] L. Beirão da Veiga, D. Mora, and G. Vacca. The Stokes complex for virtual elements with application to Navier–Stokes flows. *Journal of Scientific Computing*, 81, 11 2019. doi: 10.1007/s10915-019-01049-3.
- [3] L. Beirão da Veiga, F. Dassi, and G. Vacca. The stokes complex for virtual elements in three dimensions. *Mathematical Models and Methods in Applied Sciences*, 30(03):477–512, 2020.
- [4] C. Cherubini, S. Filippi, A. Gizzi, and R. Ruiz-Baier. A note on stress-driven anisotropic diffusion and its role in active deformable media. *Journal of Theoretical Biology*, 430(7):221–228, 2017. doi: 10.1016/j.jtbi.2017.07.013.
- [5] F. Dassi. VEM++, a C++ library to handle and play with the virtual element method, 2023. URL <https://arxiv.org/abs/2310.05748>.
- [6] F. Dassi, A. Fumagalli, A. Scotti, and G. Vacca. Bend 3d mixed virtual element method for Darcy problems. *Computers & Mathematics with Applications*, 119:1–12, 2022.
- [7] P. Grigoreva, E. N. Vilchevskaya, and W. H. Müller. *Stress and Diffusion Assisted Chemical Reaction Front Kinetics in Cylindrical Structures*, pages 53–72. Springer International Publishing, Cham, 2019.
- [8] R. Khot, A. E. Rubiano, and R. Ruiz-Baier. Robust virtual element methods for coupled stress-assisted diffusion problems. *SIAM Journal on Scientific Computing*, 1:in press, 2024.
- [9] J. Meng, L. Beirão da Veiga, and L. Mascotto. Stability and interpolation properties for stokes-like virtual element spaces. *Journal of Scientific Computing*, 94:e56, 2023.
- [10] J. D. Murray and J. D. Murray. *Mathematical Biology: II: Spatial Models and Biomedical Applications*, volume 3. Springer, 2003.
- [11] M. Taralov. *Simulation of Degradation Processes in Lithium-Ion Batteries*. Phd thesis, Technische Universität Kaiserslautern, 2015. URL <https://nbn-resolving.de/urn:nbn:de:hbz:386-kluedo-40855>.